Journal of Saudi Chemical Society (2023) 27, 101674

King Saud University

Journal of Saudi Chemical Society

www.ksu.edu.sa
www.sciencedirect.com

ORIGINAL ARTICLE

Discovery novel VEGFA inhibitors through structure-based virtual screening and verify the ability to inhibit the proliferation, invasion and migration of gastric cancer

Man Ren [a,b,1,*], Dan Li [b,c,1], Gejing Liu [a,b], Yingshi Du [a,b]

[a] Department of Geriatrics Gerontology, The First Hospital of Lanzhou University, Lanzhou 730000, Gansu, China
[b] The First Clinical Medical College, Lanzhou University, Lanzhou 730000, Gansu, China
[c] Office of National Drug Clinical Trial Institutions, The First Hospital of Lanzhou University, Lanzhou 730000, Gansu, China

Received 23 March 2023; revised 20 May 2023; accepted 9 June 2023
Available online 19 June 2023

KEYWORDS

Gastric cancer;
1, 2, 3, 4, 6-penta-o-galloyl-β- d-glucose;
VEGFA;
Molecular docking;
Molecular dynamics simulation

Abstract This paper aims to screen small molecule inhibitors 1,2,3,4,6-penta-O-galloyl-beta-D-glucose (PGG) targeting vascular endothelial growth factor A (VEGFA) through structure based virtual screening and molecular dynamics simulation, and verify the effect of anti gastric cancer.

First, Based on Traditional Chinese Medicine Systems Pharmacology Database and Analysis Platform, the candidate small-molecule compounds targeting VEGFA were screened by a molecular docking method using Computer-Aided Drug Design. Second, CCK8 was used to determine the effect of three commercially available candidate drugs on the proliferation activity of HGC27 and AGS. PGG was selected for further cell cloning, invasion, migration and apoptosis experiments. Finally, the complex system of three compounds and VEGFA was analyzed by molecular dynamics simulation.

According to the ranking of the scoring function, the selected small molecular compounds are PGG, 2,3,4,6-tetra-O-galactosyl-D-glucopyranoside, rutin, quercetin-5,3-d-galactoside and 1F-Fructofuranosylnystose (1FF). CCK8 showed that PGG had the best inhibitory effect on the proliferation of AGS and HGC27 cells, and it was concentration and time dependent. Treatment of AGS and HGC27 with IC_{50} PGG can significantly inhibit the cloning of HGC27 and AGS, block their invasion and migration, and induce their apoptosis. Molecular dynamics simulation

* Corresponding author at: Department of Geriatrics Gerontology, The First Hospital of Lanzhou University, No.1 West Donggang Road, Lanzhou 730000, Gansu, China.
E-mail address: renman1983@163.com (M. Ren).
[1] These authors contributed equally to this research.

Peer review under responsibility of King Saud University. Production and hosting by Elsevier.

Production and hosting by Elsevier

https://doi.org/10.1016/j.jscs.2023.101674

experiments showed that the binding of PGG to VEGFA target protein was better than that of other two small molecular compounds, which was consistent with the results of molecular docking and biological activity experiments.

1. Introduction

Gastric cancer is the fourth most common cancer globally [1]. China has the highest incidence rate of gastric cancer in the world, accounting for 7.7% of all cancer deaths [2]. Chemotherapy plays a leading role in the management of advanced gastric cancer [3]. Because Chinese herbal medicine has many targets and poses less of a threat to normal cells, it has unique advantages in alleviating tumours, reducing adverse reactions of chemotherapy, improving quality of life, prolonging survival time, etc [4]. Therefore, it is significant to identify relevant traditional Chinese medicine components with anti-tumour effects for high-efficiency targeting [5].

Vascular endothelial growth factor A (VEGFA) can promote angiogenesis, increase vascular permeability and extracellular matrix degeneration [6], so it plays an important role in inducing vascular proliferation and supporting tumor growth and metastasis. Targeting VEGFA against angiogenesis has been recognized as one of the most promising methods for clinical tumour treatment [7,8,9].

Based on Traditional Chinese Medicine Systems Pharmacology Database and Analysis Platform (TCMSP), this study used the molecular docking method of Computer-Aided Drug Design (CADD) to screen small molecule candidate compound 1,2,3,4,6-penta-O-galacyl- β- D-glucose (PGG) (Fig. 1) targeting VEGFA. In recent years, multiple studies have shown that PGG has great potential in the fight against cancer [10]. For example, PGG has cytoprotection on oxidative damage of human hepatoma cells [11]. In addition, PGG has anti proliferative and anti metastatic effects on colorectal cancer [12]. This study aims to reveal that CADD has certain theoretical guidance significance for screening small molecule compounds targeting VEGFA, such as PGG, and to clarify the role of PGG in gastric cancer.

2. Materials and methods

2.1. Reagents

PGG, rutin and 1F- Fructofuranoside (1FF) were purchased from Nantong Feiyu Biotechnology Co., Ltd. Jiangsu Province, China. Human gastric cancer cell lines AGS and HGC27 were provided by Zhejiang Meisen Cell Technology Co., Ltd. Dulbecco's Modified Eagle Medium/Nutrient Mixture F-12 (DMEM) and foetal bovine serum (FBS) was purchased from Gibco. A CCK8 kit (No. C0037), Annexin V-FITC (No. C1062S) apoptosis detection kit and Crystal violet dye solution (No. C0121-100 Ml) was purchased from Beyotime. Trypsin (No. T1300), Matrigel (No. 356234), and bovine serum albumin (BSA, No. pc0001) were purchased from Beijing sulaibao Technology Co., Ltd China. Penicillin Streptomycin Solution (No. SV30010) was purchased from Hyclone.

2.2. VEGFA protein pre-treatment

The VEGFA protein structure was downloaded from the Protein Data Bank database and the protein code (3QTK) was saved in Protein Data Bank format. First, the Protein Prep module of Schrödinger software was used to complete the side chain, protonation, dehydration, hydrogenation, and other treatments of the missing residues of the protein. Under the condition of the OPLS2005 force field, the ligand position in 3QTK was designated as the docking site of small molecules within the pH range (pH = 7.0 ± 2.0). The Receiver Grid Generation module was used to generate the lattice file required for virtual screening by using the default program parameters for the crystal structure, producing small molecules with multiple conformations.

2.3. Virtual screening based on molecular docking

Virtual screening was carried out using the virtual screening workflow in the Maestro module of Schrödinger software [13]. First, the Qik Prop module was used to preliminarily screen small-molecular compounds. Any that did not have drug-forming physical and chemical properties according to Lipinski rules were filtered and eliminated, and only those that met the drug-like rules were retained. After that, Glide [14] was used for step-by-step screening, in which high-throughput virtual screening retained the top 10% compounds, standard precision retained the top 10% compounds, and additional precision retained the top 10% compounds [15].

2.4. Cell culture

AGS and HGC27 cells were cultured in a medium supplemented with 10% FBS and incubated at 37℃ in a 5% CO_2

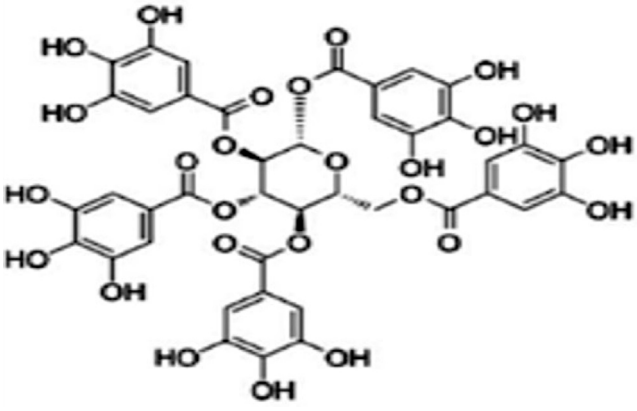

Fig. 1 Chemical structural of 1,2,3,4,6-penta-o-galloyl-β-d-glucose.

incubator. When the cells grew to the logarithmic growth stage, they were digested and collected for subsequent experiments.

2.5. CCK8 assay

Cell suspensions (5×10^5 cells/well) were inoculated in a 96-well plate. PGG was added for 48 h after the cells completely adhered to the walls. To conduct the CCK8 experiment, different concentrations (0 μmol/L, 20 μmol/L, 30 μmol/L and 40 μmol/L) of PGG were added to the AGS and HGC27 cells for 12 h, 24 h, 36 h, 48 h, and 60 h respectively. Ten microlitres of solution was added to each hole in the CCK8 solution and incubated for 2 h. The microplate reader was used to measure the absorbance (OD) at 450 nm, and the cell inhibition rate of different treatment groups was calculated. The following formula was used: Inhibition rate = [1-(experimental group OD-blank group OD)/ (control group OD-blank group OD)] × 100%.

2.6. Annexin V and propidium iodide (PI) staining

Cells in each group were digested with 0.25% trypsin without Ethylene Diamine Tetraacetic Acid, collected after termination of digestion, and centrifuged at 1500 rpm for 5 min. The supernatant was discarded and the cells were collected. The cells were then resuspended with twice pre-cooled PBS, centrifuged at 1500 rpm for 5 min and washed. Three-hundred microlitres of binding buffer was used to suspend the cells. Annexin V-FITC labelling was performed by mixing 5 μL of Annexin V-FITC while avoiding light, and incubating the cells at room temperature for 15 min. propidiumiodide labeling was performed by adding 10 μL of propidiumiodide stain, gently mixing the cells, and incubating them at room temperature under dark conditions for 10 min. Flow cytometry was then used for detection and cell quest software was used for analysis.

2.7. Cell colony formation test

HGC27 and AGS gastric cancer cells were treated with IC_{50} PGG for 48 h. Cells from each group in the logarithmic growth period were taken to prepare the cell suspension. The cells from each group were then spread into six-well plates with 200 cells/well and then stained with crystal violet after two weeks. Photos were taken under a microscope and the formation of clones was observed.

2.8. Scratch healing test

After the treatment of HGC27 and AGS gastric cancer cells with IC_{50} PGG for 48 h, the cells in each group were digested with trypsin and counted, spread into six-well plates with 5×10^5 cells/well, and covered overnight. The cells were washed with PBS three times, the delimited cells were discarded, and the serum-free medium was added. The cells were cultivated at 37℃ in a 5% CO_2 incubator. Photos were taken to record the scratch healing at 0 h and 48 h.

2.9. Transwell test

Dilute the cell suspension with DMEM basic medium to 1×10^5/Ml. 600 μL of DMEM complete medium containing 20% FBS was added to the matching 24-well plate, placing the chamber into the holes carefully to avoid bubbles. Two-hundred microlitres of fully mixed cell suspension was added to the chamber, and the cells were placed in the incubator for 24 h. The cells were washed with PBS and fixed with 4% anhydrous methanol for 30 min, dyed with crystal violet for 20 min, and rinsed with PBS to remove the excess dye. The cells inside the chamber were then wiped with cotton swabs. Nine visual fields were randomly selected to observe the cells and take photos. Image J software was used to calculate the number of cells and sort the results, and Graphad software was used to draw pictures.

2.10. Molecular dynamics simulation

Molecular dynamics simulation of the PGG-VEGFA complex was carried out using the Amber18 software package. Proteins use the ff99SB force field parameters [16], small-molecule ligands use the gaff general force field parameters, and the antechamber module [17] was used to fit the electrostatic potential to get the partial charge of the atom. The protein small-molecule complex was loaded into the tleap module [18] and hydrogen atoms and antagonistic ions were automatically added to neutralize the charge. The TIP3P dominant water model [19] was selected and periodic boundary conditions were set. The workflow of the molecular dynamics simulation included four steps: energy minimization, heating, equilibrium, and production dynamics simulation [20]. First, the heavy atoms of proteins (and small molecules) were constrained, and 5000 steps (including 2500 steps of the steepest descent method combined with 2500 steps of the conjugate gradient method) energy minimization was performed on the water molecules and protein side chains. Then, the system was slowly heated to 310 K within 100 ps. During the heating process, the simple harmonic force of 5.0 kcal/(mol·Å2) was used to limit the protein. Langevin thermostatic controller with a coupling coefficient of 2.0 ps^{-1} was used to control the temperature. After heating, the study system was balanced six times under the NPT ensemble, and the limiting forces of the system were 5.0, 2.0, 1.0, 0.5, 0.1 and 0 kcal/(mol·Å2), respectively. Among these, the simulation duration of the first five times was 100 ps, and 500 ps for the sixth time, with a total balance of 1 ns. Finally, a 250-ns molecular dynamics simulation of the system was carried out under the NPT ensemble. The time step was set to 2 fs. In the process of simulation, the SHAKE algorithm [21] was used to limit the bond length containing hydrogen atoms. The particle mesh Ewald method was used to deal with long-range electrostatic interactions, and the non-bond truncation distance was set to 10 Å. The MMPBSA.py script was used to calculate the contribution of ligand and protein.

2.11. Data Analysis

All data are presented as the mean ± SD. One-way ANOVA was used to compare the differences between the groups. All

statistical analyses were completed by Grahpad7.0 software. Statistical differences between the groups was set at $p < 0.05$.

3. Results

3.1. Analysis of molecular docking results

The optimized VEGFA protein kinase structure was used in the Traditional Chinese Medicine Systems Pharmacology Database and Analysis Platform for virtual screening through molecular docking. When selecting compounds, we mainly referred to the ranking of the docking score and glide score, comprehensively considering the binding mode and characteristics of the ligand and receptor protein, relative molecular weight, molecular surface area, lipid water partition coefficient, compound skeleton structure, and other factors. The five compounds screened were PGG, rutin, 1FF, 2,3,4,6-tetra-o-gal loyl-d-glucopyranoside, and Quercetin-5,3-di-D-galactoside.

Table 1 Docking scoring function of VEGFA and five candidate compounds in Traditional Chinese Medicine Systems Pharmacology Database and Analysis Platform.

Database	small moleculecompounds	Docking scoring function with VEGFA	source
T	2,3,4,6-tetra-o-galloyl-d-glucopyranoside	−12.132	Ampelopsis japonica
C	1,2,3,4,6-penta-O-galloyl-beta-D-glucose	−13.327	Ampelopsis japonica
M	Quercetin-5,3-di-galactoside	−12.491	Polydatin
S	rutin	−12.134	Hedyotis diffusa
P	1F-Fructofuranosylnystose	−11.999	Morinda

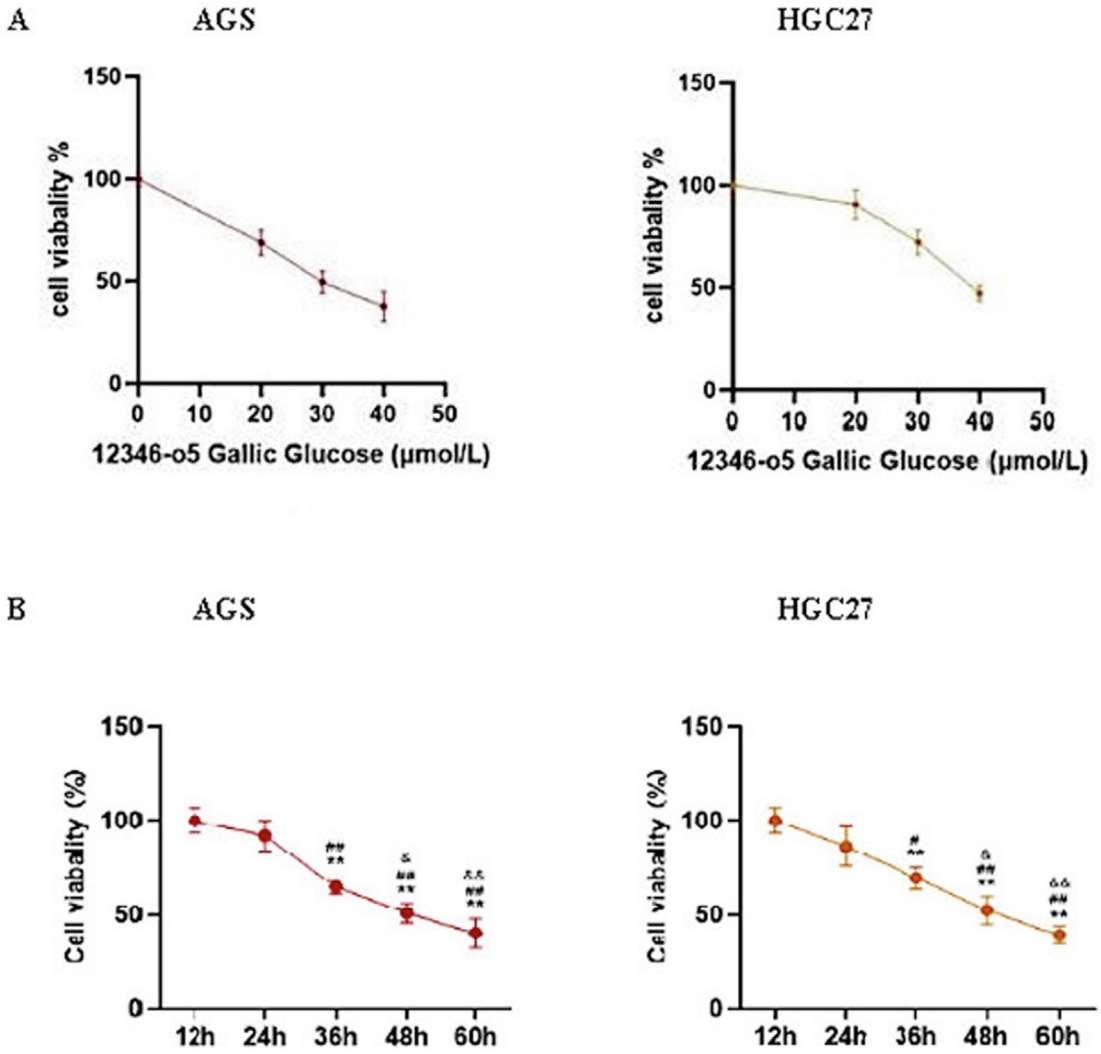

Fig. 2 Effects of 1,2,3,4,6-penta-O-galloyl-beta-D-glucose on proliferation in AGS and HGC27 gastric cancer cells (A). gastric cancer cells (5×10^5 cells/well) were treated with 1,2,3,4,6-penta-O-galloyl-beta-D-glucose (0, 20, 30, 40 μmol/L), then cell viability was measured by CCK8 assay. **(B)** The gastric cancer cells (5×10^5 cells/well) were treated with PGG (30.19 μmol/L and 38.87 μmol/L) for indicated time intervals (12, 24, 36, 48, 60 h).

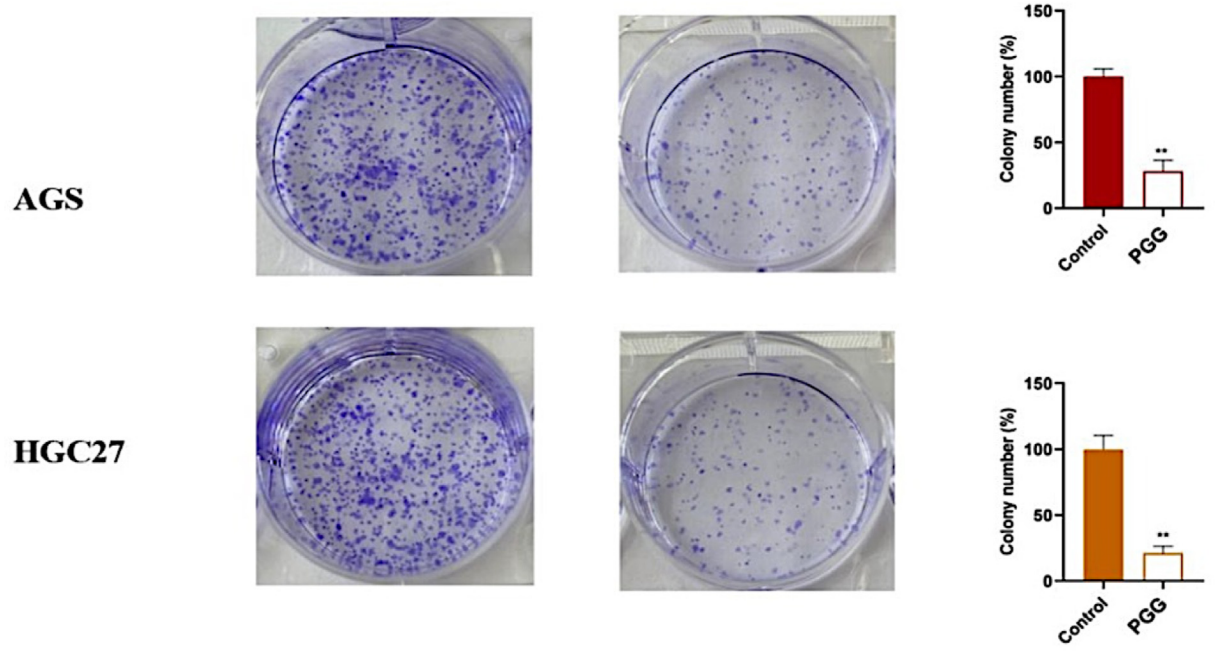

Fig. 3 gastric cancer cells (200 cells/well) were treated with IC_{50} 1,2,3,4,6-penta-O-galloyl-beta-D-glucose for 48 h.

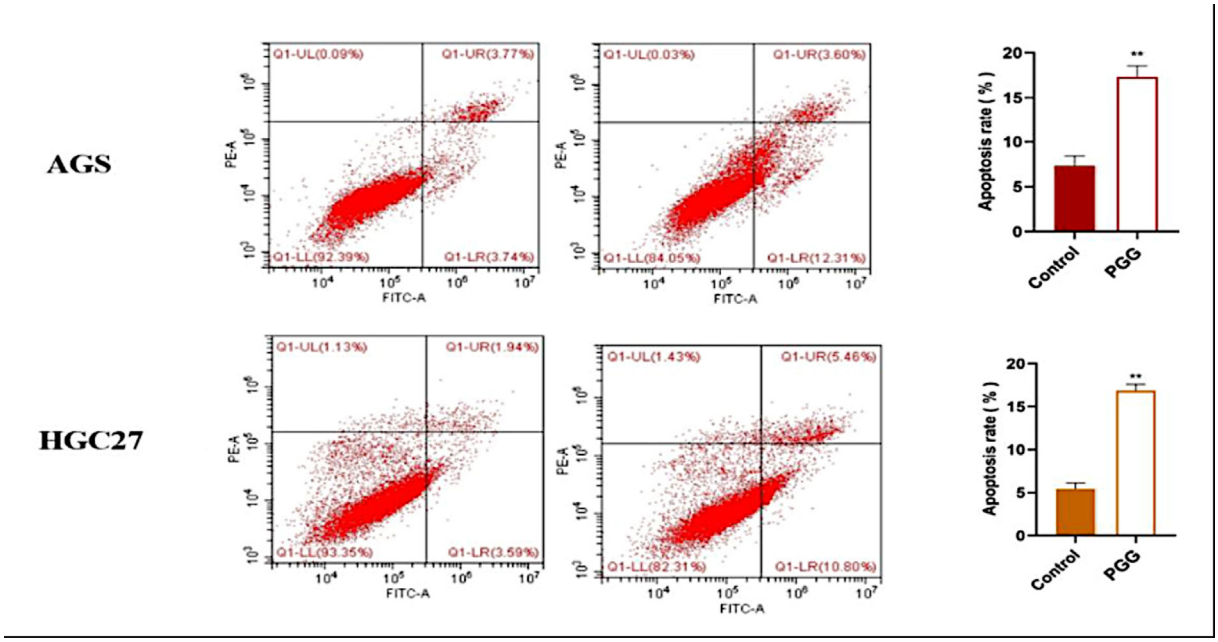

Fig. 4 Effects of 1,2,3,4,6-penta-O-galloyl-beta-D-glucose on apoptotic cell death in gastric cancer cells. IC_{50} 1,2,3,4,6-penta-O-galloyl-beta-D-glucose treated cells were incubated with Annexin V-FITC and PI for 15 min. Apoptosis was measured by flow cytometric analysis. All experiments were performed independently at least three times and representative data has been shown.

The greater the absolute value of the docking score with VEGFA, the better the binding effect. PGG scored the highest, at −13.327 (Table 1).

3.2. PGG reduced the viability of gastric cancer cell lines

The viability results of AGS and HGC27 cells treated with PGG detected by CCK8 are shown in Figs. 2 and 3. Compared with the 0 μmol/L group, the cell viability of the other groups decreased in a dose-dependent manner. The IC_{50} value of the AGS cells treated with PGG was 30.19 μmol/L and that of the HGC27 cells was 38.87 μmol/L (Fig. 2**A**).

Compared with the 12 h group, there was no significant difference in cell viability at 24 h; however, the cell viability decreased significantly at 36 h, 48 h, and 60 h. The longer the duration, the more obvious the decline in cell viability

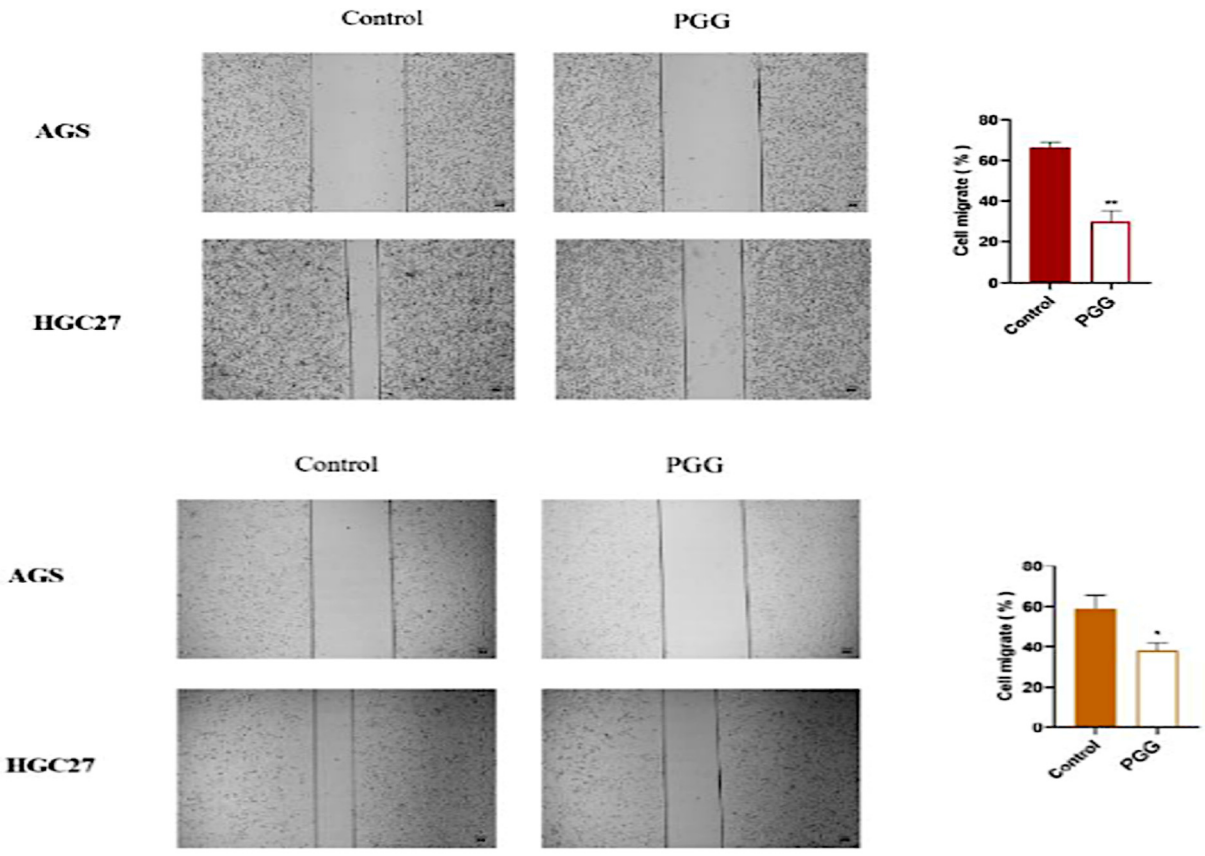

Fig. 5 Effects of 1,2,3,4,6-penta-O-galloyl-beta-D-glucose on migration of gastric cancer cells The gastric cancer cells (5×10^5 cells/well) were treated with IC_{50} PGG for 48 h, and the area enclosed by two black lines represents the measured scratch area.

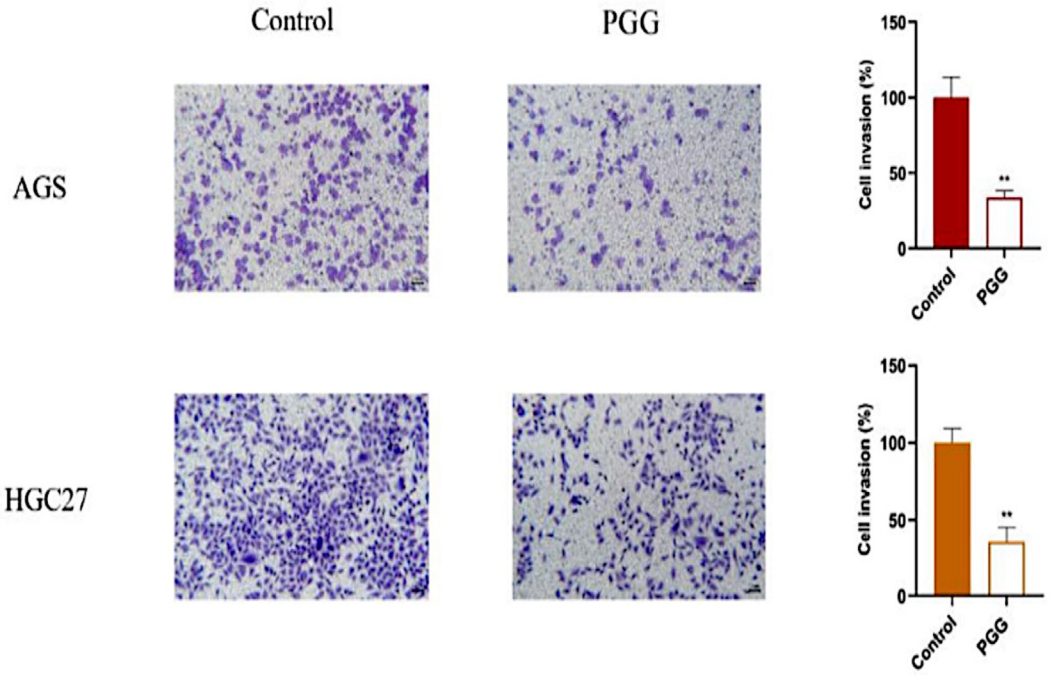

Fig. 6 Effects of 1,2,3,4,6-penta-O-galloyl-beta-D-glucose on invasion of gastric cancer cells The gastric cancer cells (1×10^6 cells/well) were treated with IC_{50} PGG for 48 h.

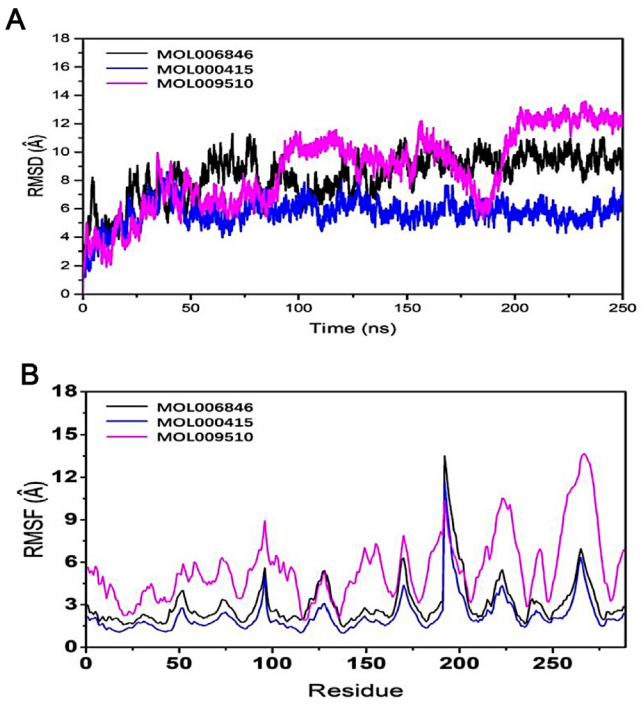

Fig. 7 **(A)** RMSD of protein skeleton atoms**(Cα, N, O, C) (B)** RMSF of protein residues Cα.

(Fig. 2**B)**. We selected IC_{50} PGG treat AGS and HGC27 cells for 48 h for follow-up experiments.

3.3. PGG can reduces the cloning of gastric cancer cell lines

The cloning results of AGS and HGC27 cells treated with IC_{50} PGG for 48 h are shown in Fig. 3. Compared with control group, the number of cell clones in the PGG group decreased significantly.

3.4. PGG stimulated the apoptotic cell death in gastric cancer cell lines

The apoptotic results of AGS and HGC27 cells treated with IC_{50} PGG for 48 h were detected by flow cytometry, as shown in Fig. 4. Compared with the control group, the apoptotic rate of the PGG group was significantly higher **(**Fig. 4**)**.

3.5. PGG can prevents gastric cancer cell lines migration

The migration ability of AGS and HGC27 cells treated with IC_{50} PGG for 48 h was tested by the scratch healing test. Compared with control group, the cell migration ability of the PGG group decreased significantly **(**Fig. 5**)**.

3.6. PGG can blocks gastric cancer cell lines from invading

The invasion ability of AGS and HGC27 cells treated with IC_{50} PGG for 48 h was detected by the Transwell experiment. Compared with the control group, the invasion ability of the PGG group decreased significantly **(**Fig. 6**)**.

3.7. Analysis of molecular dynamics simulation

In order to monitor whether the simulation system reaches equilibrium, we calculated the root mean square deviation (RMSD) of the protein skeleton atoms (Cα, N, O, C). Fig. 7A shows the RMSD as a function of simulation time. Fig. 7B shows that the PGG-VEGFA complex system converges from about 150 ns and tends to be stable.

In order to study PGG small molecules acting on receptor proteins, we calculated the contribution between PGG small molecules and protein receptors using the MM/GBSA method (Table 2). The contribution of PGG small molecules to protein receptors is −48.3825 kcal/mol, which proves that PGG small molecules can bind to protein receptors. Van der Waals effects and electrostatic interactions are conducive to the binding of PGG small molecules to protein receptors, with the former interactions slightly more dominant.

In order to identify the important residues of PGG small molecules interacting with protein receptors, we performed residue energy decomposition (Fig. 8A). Residues with an energy contribution of more than 1.5 kcal/mol were considered effective. It can be seen that A-chain ASP27 and ILE39, D-chain LYS100, and F-chain VAL8, LYS9, PHE10, ARG98, PRO99, and LYS101 all provide higher energy contributions, with residues in the F chain contributing more than residues in the A and D-chains, indicating that residues in the F-chain play a greater role in the binding of PGG to protein receptors.

Although van der Waals forces provide the main energy contribution to binding, hydrogen bond interactions between proteins and ligands are also very important for the study of the binding mechanism. Therefore, we also monitored the hydrogen bond interaction between small-molecule ligands and proteins in the complex system during the 250 ns simulation process (Fig. 9). We set the hydrogen bond standard as the distance between the hydrogen bond donor atom (D) and the hydrogen bond acceptor atom (A) < 3.0 Å and the bond angle A...H-D greater than 120.0°; as long as these standards were met, the small-molecule ligands in the complex system were forming hydrogen bond interactions with proteins. In Fig. 9, the hydrogen bonds formed between small molecules and F-chain PRO99 residues account for more than 80%, indicating that these hydrogen bond interactions are very important for the inhibitory activity of the compounds (see Fig. 10).

In order to intuitively show the interaction between PGG small molecules and proteins, we analyzed the free energy

Table 2 Contribution of 1,2,3,4,6-penta-o-galloyl-beta-d-glucose-vegfa.

Complex	Contribution				
	ΔEle	ΔEvdw	ΔEgb	ΔEsurf	ΔGbind
VEGFA-1,2,3,4,6-penta-O-galloyl-beta-D-glucose	−43.9479	−68.4391	76.0750	−12.0705	−48.3825

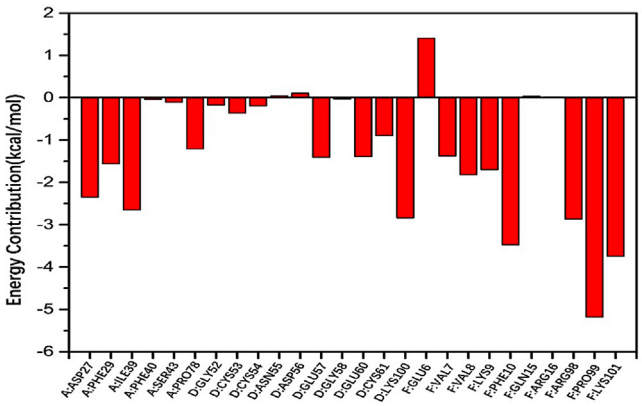

Fig. 8 A Decomposition diagram of binding free energy residues of 1,2,3,4,6-penta-O-galloyl-beta-D-glucose-VEGFA.

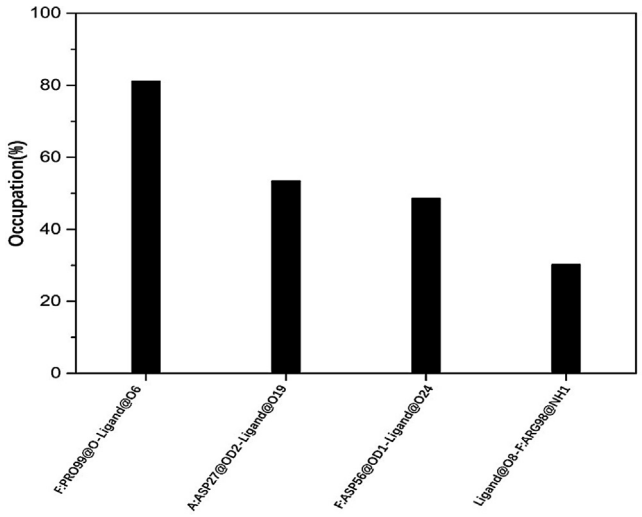

Fig. 9 Hydrogen bond occupancy of 1,2,3,4,6-penta-O-galloyl-beta-D-glucose-VEGFA.

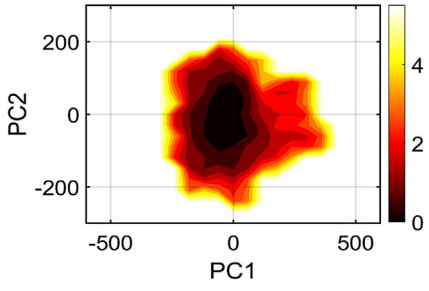

Fig. 10 Binding free energy hydrazine diagram of 1,2,3,4,6-penta-O-galloyl-beta-D-glucose-VEGFA.

hydrazine diagram of the trajectory, and extracted low-energy conformations to show the interaction between small molecules and proteins (Fig. 11).

Finally, we analyzed the conformation of PGG at the active site of VEGFA. As shown in Fig. 11, the structure of small molecule PGG can be seen as the side chain containing benzene ring inserted into the protein pocket with the epoxy six-membered ring as the center, and closely combined with the target protein. Although it is different from the "T" type inserted into the protein pocket in the initial virtual screening, in the simulation process, we analyze that PGG is combined by a more compact multiple side chains inserted into the pocket at the same time, and the small molecule is connected by the A chain ILE39, D chain CYS53 Surrounded by hydrophobic amino acids such as CYS54 and F chain VAL7, each side chain of the small molecule can combine with the protein to achieve a stable binding state. At the same time, the small molecule and A chain ASP27, F chain ASP56, PRO99, LYS101 form hydrogen bond interaction.

4. Discussions

Traditional Chinese medicine has a wide range of sources, rich chemical components, and reduced adverse reactions, and is easily accepted by the human body, which explains why it has attracted increasing attention from researchers both locally and globally [22]. Currently, the screening and exploration of new small-molecule therapeutic drugs from traditional Chinese medicine for disease targets has become a hot topic of research [23].

PGG is a natural polyphenolic compound, derived from multiple medicinal plants, including Ampelopsis japonica, Schinus terebinthifolius, Rhus chinensis Mill., Paeonia lactiflora Pall., etc [24]. PGG reportedly possesses various biological and pharmacologic activities, including anti-cancer, anti-oxidative, anti-inflammatory, anti-coagulation, anti-angiogenesis, radio-protective, and neuroprotective properties [25]. Presently, there is no research on the application of PGG in the treatment of gastric cancer, neither locally, nor abroad.

In this study, the Glide docking-based virtual screening and kinase inhibition assay were conducted to preliminary screen five VEGFA inhibitors from the Traditional Chinese Medicine Systems Pharmacology Database and Analysis Platform database. We calculated the docking scoring function of these small-molecule candidate compounds with VEGFA and PGG scored the highest. We tested the CCK8 activity of three candidate compounds available on the market to verify whether they have a inhibitory effect on gastric cancer. The IC_{50} value of AGS cells treated with PGG was 30.19 μmol/L, and that of the HGC27 cells was 38.87 μmol/L. Comparatively, the IC_{50} value of rutin-treated AGS cells was 280.5 μmol/L and that of HGC27 cells was 300.5 μmol/L. Even when 1F-Fructofuranosylnystose was administered at high doses (320 μmol/L), it still had no obvious effect, so it was considered to have little significance in the inhibition of the activity of gastric cancer cells. The results showed that PGG had the strongest inhibitory effect on the activity of gastric cancer cells compared to the other two small-molecular compounds, which was consistent with the molecular docking results.

Using different concentrations of PGG to treat AGS and HGC27 gastric cancer cells at different times found that each concentration of PGG can inhibit cell proliferation in a dose-dependent manner. In addition, the treatment of gastric cancer cells with IC_{50} PGG for 48 h could prevent the

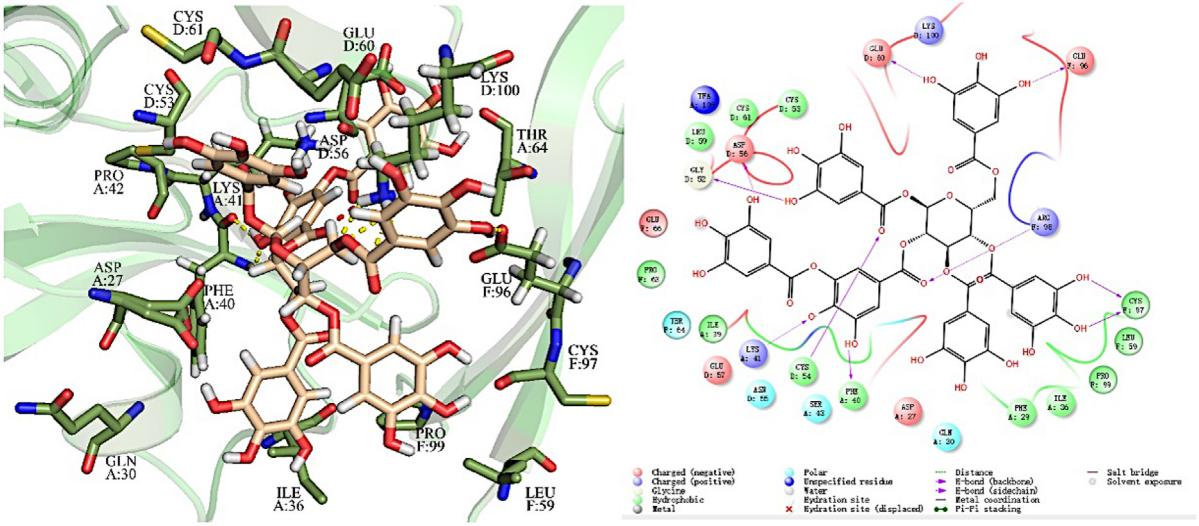

Fig. 11 The conformation of 1,2,3,4,6-penta-O-galloyl-beta-D-glucose at the active site of VEGFA (gray represents protein A-chain, purple represents protein D-chain, orange represents protein F-chain; green represents small molecules; yellow dotted line represents hydrogen bondinteraction).

formation of cell clones and induce cell apoptosis. The migration and invasion of gastric cancer cells is an important reason for the proliferation and recurrence of gastric cancer. The scratch healing and transwell test showed that the treatment of gastric cancer cells with IC_{50} PGG for 48 h reduced their migration. Therefore, PGG can inhibit the invasion of cancer cells and reduce the recurrence and proliferation of cancer. This study showed that there was almost no significant difference in all phenotypic results of AGS and HGC27 with IC_{50} PGG treatment for 48 h, but several phenotypes, such as migration, were slightly more obvious in AGS than in HGC27; however, there was no statistical difference (p greater than 0.05).

Finally, we used conventional molecular dynamics simulation to explore the interaction mechanism between the PGG, rutin, 1F-Fructofuranosylnystose and VEGFA target protein. We found that van der Waals interaction played an important role between the three compounds and the target.

Especially, the PGG small molecule is surrounded by hydrophobic amino acids such as A-chain ILE39, D-chain CYS53 and CYS54, and F-chain VAL7. The structure of the small molecule can be viewed by taking the epoxy six-membered ring as the centre, with the side chain containing a benzene ring inserted into the protein pocket, which closely combines with the target protein. The hydroxyl groups on multiple benzene rings in the PGG small molecule form hydrogen bond interactions with A-chain ASP27 and F-chain PHE10, ASP56, PRO99, LYS101, etc. At this time, PGG binds in a more compact way with multiple side chains inserted into the pocket simultaneously, so that each side chain of the small molecule can bind to the protein to achieve a stable binding state. We optimized the structure of the PGG compound to enhance the hydrogen bond interaction with the residues mentioned for the A and F chains to improve the inhibitory activity. The results showed that the combination of PGG-VEGFA composite system was the most stable compared with the other two composite systems. This is also consistent with our previous phenotypic experimental results.

However, our research has some limitations. First, we only studied the drug in vitro and did not conduct any in vivo experiments. Second, although we have proved that the studied drug has anti-tumour effects, and used molecular physics to clarify the mechanism, tumour is a complex whole, so further research is needed to clarify the specific molecular mechanism of anti-tumour drugs from a biological point of view.

5. Conclusions

We hope our research provides some theoretical guidance for the rational design of virtual screening methods and effective new VEGFA inhibitors. PGG can stably bind to VEGFA and inhibit the malignant biological behavior of gastric cancer cells, and could be considered a promising anti-VEGFA compound for the further development of VEGFA inhibitors for targeted therapy.

Ethic approval

The conducted research is not related to either human or animal use.

CRediT authorship contribution statement

Man Ren: Conceptualization, Methodology, Funding acquisition, Writing – original draft. **Dan Li:** Funding acquisition, Writing – review & editing. **Gejing Liu:** Data curation. **Yingshi Du:** Investigation.

Declaration of Competing Interest

This research was supported by the Natural Science Foundation of Gansu Province [grant numbers 22JR5RA930, 22JR5RA894], the talent Project of Lanzhou Science and Technology Bureau[grant numbers 2022-3-44], Projects

managed by Gansu Province Administration of Traditional Chinese Medicine [grant number GZKG-2022-54], Intra hospital fund of the First Hospital of Lanzhou University [grant number ldyyyn2021101], and Gansu Health Industry Scientific Research Project [grant number GSWSKY2022-67].

References

[1] F. Bray, J. Ferlay, I. Soerjomataram, R.L. Siegel, L.A. Torre, A. Jemal, Global cancer statistics 2018: GLOBOCAN estimates of incidence and mortality worldwide for 36 cancers in 185 countries, CA. Cancer J. Clin. 68 (2018) (2018) 394–424, https://doi.org/10.3322/caac.21492.

[2] P. Rawla, A. Barsouk, Epidemiology of gastric cancer: global trends, risk factors and prevention, Przeglad Gastroenterol. 14 (2019) 26–38, https://doi.org/10.5114/pg.2018.80001.

[3] M. Zang, Y. Zhang, B. Zhang, L. Hu, J. Li, Z. Fan, H. Wang, L. Su, Z. Zhu, C. Li, C. Yan, Q. Gu, B. Liu, M. Yan, CEACAM6 promotes tumor angiogenesis and vasculogenic mimicry in gastric cancer via FAK signaling, Biochim. Biophys. Acta BBA - Mol. Basis Dis. 1852 (2015) 1020–1028, https://doi.org/10.1016/j.bbadis.2015.02.005.

[4] C. Eveno, M. Pocard, VEGF levels and the angiogenic potential of the microenvironment can affect surgical strategy for colorectal liver metastasis, Cell Adhes. Migr. 6 (2012) 569–573, https://doi.org/10.4161/cam.23247.

[5] A.C. Ziogas, N.G. Gavalas, M. Tsiatas, O. Tsitsilonis, E. Politi, E. Terpos, A. Rodolakis, G. Vlahos, N. Thomakos, D. Haidopoulos, A. Antsaklis, M.A. Dimopoulos, A. Bamias, VEGF directly suppresses activation of T cells from ovarian cancer patients and healthy individuals via VEGF receptor Type 2, Int. J. Cancer. 130 (2012) 857–864, https://doi.org/10.1002/ijc.26094.

[6] A.W. Griffioen, V.L. Thijssen, Galectins in tumor angiogenesis, Ann. Transl. Med. 2 (2014) 90, https://doi.org/10.3978/j.issn.2305-5839.2014.09.01.

[7] E. Borcoman, C. Le Tourneau, Pembrolizumab in cervical cancer: latest evidence and clinical usefulness, Ther. Adv. Med. Oncol. 9 (2017) 431–439, https://doi.org/10.1177/1758834017708742.

[8] V. Sini, A. Cassano, D. Corsi, M. De Laurentiis, T. Gamucci, M. Mauri, G. Naso, M. Roselli, E.M. Ruggeri, G. Tonini, P. Vici, G. Zampa, P. Marchetti, Bevacizumab as first-line treatment in HER2-negative advanced breast cancer: pros and cons, Tumori. 102 (2016) 472–480, https://doi.org/10.5301/tj.5000555.

[9] N. Ferrara, VEGF and the quest for tumour angiogenesis factors, Nat. Rev. Cancer. 2 (2002) 795–803, https://doi.org/10.1038/nrc909.

[10] H.F. Dvorak, Vascular permeability factor/vascular endothelial growth factor: a critical cytokine in tumor angiogenesis and a potential target for diagnosis and therapy, J. Clin. Oncol. Off. J. Am. Soc. Clin. Oncol. 20 (2002) 4368–4380, https://doi.org/10.1200/JCO.2002.10.088.

[11] E. Van Cutsem, S. de Haas, Y.-K. Kang, A. Ohtsu, N.C. Tebbutt, J. Ming Xu, W. Peng Yong, B. Langer, P. Delmar, S.J. Scherer, M.A. Shah, Bevacizumab in combination with chemotherapy as first-line therapy in advanced gastric cancer: a biomarker evaluation from the AVAGAST randomized phase III trial, J. Clin. Oncol. Off. J. Am. Soc, Clin. Oncol. 30 (2012) 2119–2127, https://doi.org/10.1200/JCO.2011.39.9824.

[12] H. Yang, G.-G.-L. Yue, P.-C. Leung, C.-K. Wong, Y.-J. Zhang, C.-B.-S. Lau, Anti-metastatic effects of 1,2,3,4,6-Penta-O-galloyl-β-D-glucose in colorectal cancer: Regulation of cathepsin B-mediated extracellular matrix dynamics and epithelial-to-mesenchymal transition, Pharmacol. Res. 184 (2022), https://doi.org/10.1016/j.phrs.2022.106457 106457.

[13] A. Jakalian, D.B. Jack, C.I. Bayly, Fast, efficient generation of high-quality atomic charges. AM1-BCC model: II. Parameterization and validation, J. Comput. Chem. 23 (2002) 1623–1641, https://doi.org/10.1002/jcc.10128.

[14] V. Hornak, R. Abel, A. Okur, B. Strockbine, A. Roitberg, C. Simmerling, Comparison of multiple Amber force fields and development of improved protein backbone parameters, Proteins. 65 (2006) 712–725, https://doi.org/10.1002/prot.21123.

[15] J. Wang, R.M. Wolf, J.W. Caldwell, P.A. Kollman, D.A. Case, Development and testing of a general amber force field, J. Comput. Chem. 25 (2004) 1157–1174, https://doi.org/10.1002/jcc.20035.

[16] X. Liu, D. Shi, S. Zhou, H. Liu, H. Liu, X. Yao, Molecular dynamics simulations and novel drug discovery, Expert Opin. Drug Discov. 13 (2018) 23–37, https://doi.org/10.1080/17460441.2018.1403419.

[17] T. Xie, J. Yu, W. Fu, Z. Wang, L. Xu, S. Chang, E. Wang, F. Zhu, S. Zeng, Y. Kang, T. Hou, Insight into the selective binding mechanism of DNMT1 and DNMT3A inhibitors: a molecular simulation study, Phys. Chem. Chem. Phys. PCCP. 21 (2019) 12931–12947, https://doi.org/10.1039/c9cp02024a.

[18] X. Kong, H. Sun, P. Pan, S. Tian, D. Li, Y. Li, T. Hou, Molecular principle of the cyclin-dependent kinase selectivity of 4-(thiazol-5-yl)-2-(phenylamino) pyrimidine-5-carbonitrile derivatives revealed by molecular modeling studies, Phys. Chem. Chem. Phys. PCCP. 18 (2016) 2034–2046, https://doi.org/10.1039/c5cp05622e.

[19] P. Pan, H. Yu, Q. Liu, X. Kong, H. Chen, J. Chen, Q. Liu, D. Li, Y. Kang, H. Sun, W. Zhou, S. Tian, S. Cui, F. Zhu, Y. Li, Y. Huang, T. Hou, Combating Drug-Resistant Mutants of Anaplastic Lymphoma Kinase with Potent and Selective Type-I1/2 Inhibitors by Stabilizing Unique DFG-Shifted Loop Conformation, ACS Cent. Sci. 3 (2017) 1208–1220, https://doi.org/10.1021/acscentsci.7b00419.

[20] H. Liu, X. An, S. Li, Y. Wang, J. Li, H. Liu, Interaction mechanism exploration of R-bicalutamide/S-1 with WT/W741L AR using molecular dynamics simulations, Mol. Biosyst. 11 (2015) 3347–3354, https://doi.org/10.1039/c5mb00499c.

[21] H. Liu, R. Han, J. Li, H. Liu, L. Zheng, Molecular mechanism of R-bicalutamide switching from androgen receptor antagonist to agonist induced by amino acid mutations using molecular dynamics simulations and free energy calculation, J. Comput. Aided Mol. Des. 30 (2016) 1189–1200, https://doi.org/10.1007/s10822-016-9992-2.

[22] H. Liu, L. Wang, J. Tian, J. Li, H. Liu, Molecular Dynamics Studies on the Enzalutamide Resistance Mechanisms Induced by Androgen Receptor Mutations, J. Cell. Biochem. 118 (2017) 2792–2801, https://doi.org/10.1002/jcb.25928.

[23] Y. Matsunaga, H. Fujisaki, T. Terada, T. Furuta, K. Moritsugu, A. Kidera, Minimum free energy path of ligand-induced transition in adenylate kinase, PLoS Comput. Biol. 8 (2012) e1002555.

[24] R. Kant, C.-K. Lu, H.M. Nguyen, H.-H. Hsiao, C.-J. Chen, H.-P. Hsiao, K.-J. Lin, C.-C. Fang, C.-H. Yen, 1,2,3,4,6 penta-O-galloyl-β-D-glucose ameliorates high-fat diet-induced nonalcoholic fatty liver disease and maintains the expression of genes involved in lipid homeostasis in mice, Biomed. Pharmacother. Biomedecine Pharmacother. 129 (2020), https://doi.org/10.1016/j.biopha.2020.110348 110348.

[25] J. Zhang, L. Li, S.-H. Kim, A.E. Hagerman, J. Lü, Anti-cancer, anti-diabetic and other pharmacologic and biological activities of penta-galloyl-glucose, Pharm. Res. 26 (2009) 2066–2080, https://doi.org/10.1007/s11095-009-9932-0.